We express our sincere gratitude to your insightful and constructive comments. Please find below our point-by-point replies. All the comments are presented in black text and the corresponding replies are highlighted in blue.

The authors use a fully coupled climate model to evaluate the response of permafrost under temperature stabilization and overshoot scenarios. The methods appear rigorous, and the manuscript is well-written. However, the manuscript could be improved by discussing the implications of some of the feedbacks being modeled. Substantial revisions to some sections of the text and figures could further improve the overall clarity of the manuscript and link it more directly to existing literature.

Major comments:

Line 92 and throughout: Yedoma represents a significant, deep proportion of the permafrost carbon stock in some regions and was formed over extremely long timescales. Given the focus on differences between overshoot and stabilization scenarios, a greater discussion of this limitation could be included in the methods and conclusions.

We appreciate your insightful comment. The UVic ESCM v2.10 simulates permafrost carbon only in the top six layers (to a depth of 3.35 m), and therefore omits soil carbon stored in the deep deposits of Yedoma regions. As a result, we cannot directly estimate the impacts of temperature overshoot on deep Yedoma carbon, or compare these changes relative to stabilization scenarios. To address this limitation, we analyzed the average and maximum active layer thickness (ALT) in Yedoma regions between the overshoot and stabilization scenarios simulated in this study. Using differences in ALT as a proxy to infer the potential impacts on deep Yedoma carbon (Figure R1). To clarify this point, we have added the following paragraph to Section "4 Conclusions and Discussion":

"Yedoma deposits represent a significant deep carbon reservoir and are widespread across Siberia, Alaska, and the Yukon region of Canada, having primarily formed during the late Pleistocene, especially in the late glacial period. These deep, perennially frozen sediments are particularly ice-rich, and the freeze-locked organic matter in such deposits can be re-mobilized on short time-scales, representing one of the most vulnerable permafrost carbon pools under future warming scenarios (Schuur et al., 2015; Strauss et al., 2017). According to Zimov et al. (2006), these perennially frozen Yedoma sediments cover more than 1 million km^2, with an average depth of approximately 25 m. Recent estimates place the organic carbon stock in Yedoma deposits at 213 ± 24 PgC, constituting a significant portion of the total permafrost carbon pool (Strauss et al., 2017). However, the UVic ESCM v2.10 utilized in this study simulates permafrost carbon only within the top 3.35 m of soil, limiting our ability to directly assess the impacts of temperature overshoot on deep Yedoma carbon. Considering their ice-rich nature and potential susceptibility to rapid-thaw processes, we analyzed the average and maximum active layer thickness (ALT) in Yedoma regions (Strauss et al., 2021, 2022) under the simulated scenarios to approximate potential impacts. We find that the average ALT in Yedoma regions remains below 1 m in all stabilization and overshoot scenarios, while the maximum ALT rarely exceeds 3.35 m in overshoot scenarios but does exceed this depth in some stabilization scenarios. However, in all scenarios, the maximum ALT does not

exceed 6 m, which is relatively shallow compared to the average depth (~25 m) of Yedoma deposits. Therefore, the impact of overshoot scenarios on deep Yedoma carbon is likely minor relative to stabilization scenarios."

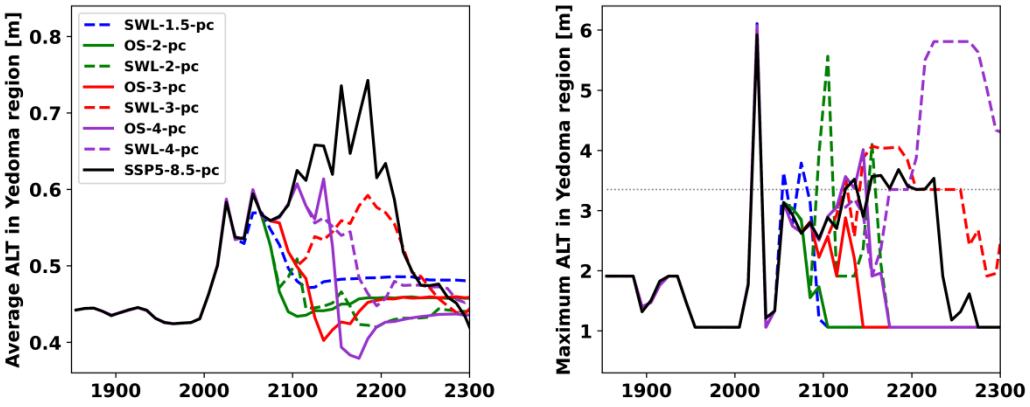

Figure R1. Timeseries of annual (a) average and (b) maximum active layer thickness (ALT) in Yedoma regions under overshoot (colored solid lines) and stabilization (colored dashed lines) scenarios at 1.5 °C (blue), 2.0 °C (green), 3.0 °C (red), and 4 °C (purple) GWLs, as well as the SSP5-8.5 scenario (black solid line). Results represent the ensemble median of 250 simulations. The Yedoma region mask used in this analysis is based on the Ice-Rich Yedoma Permafrost Database Version 2 (IRYP v2) (Strauss et al., 2021, 2022; https://doi.org/10.1594/PANGAEA.940078).

Line 90 – 103: More background on the UVICC ESM permafrost carbon model, validation, and perturbed parameter approach would be particularly useful to readers.

Thank you for your valuable suggestion. To improve clarity and provide a more comprehensive background, we have made the following revisions to this section:

"The UVic ESCM model represents the terrestrial subsurface with 14 layers, extending to a total depth of 250.3 m to correctly capture the transient response of permafrost on centennial timescales. The top eight layers (10.0 m) are involved in the hydraulic cycle, while the deeper layers are modeled as impermeable bedrock (Avis et al., 2011). The carbon cycle is active in the top six layers (3.35 m), where organic carbon from litterfall, simulated by the TRIFFID vegetation model, is allocated to soil layers with temperatures above 1 °C according to an exponentially decreasing function with depth. If all soil layers are below 1 °C, the organic carbon is added to the top soil layer. The soil respiration is calculated for each layer individually as a function of temperature and moisture, but the respiration ceases when the soil layer temperature falls below 0 °C (Meissner et al., 2003; Mengis et al., 2020). In regions where permafrost exists—defined as areas where soil temperature remains below 0°C for at least two consecutive years—the model applies a revised diffusion-based cryoturbation scheme to redistribute soil carbon within the soil column. The permafrost carbon is generated when soil carbon is transported across the permafrost table. Compared to the original diffusion-based cryoturbation scheme proposed by Koven et al. (2009), the revised cryoturbation scheme calculates carbon diffusion using an effective carbon

concentration that incorporates the volumetric porosity of the soil layer, rather than the actual carbon concentration, thereby resolving the disequilibrium problem of the permafrost carbon pool during model spin-up (MacDougall and Knutti, 2016). Notably, the UVic ESCM v2.10 does not include a methane production module, meaning that soil carbon emissions to the atmosphere are limited to CO_2. A more detailed description of the UVic ESCM's permafrost carbon parameterization scheme and its simulated permafrost carbon characteristics can be found in MacDougall and Knutti (2016)."

Model validation has been incorporated into the first paragraph in Section "3 Results". The added content is:

"The UVic ESCM v2.10 reliably simulates historical temperature changes, permafrost area, and the partitioning of anthropogenic carbon emissions among the atmosphere, ocean and land. During the period 2011–2020, the model estimated a GSAT increase of 1.14 [1.13 to 1.15] °C relative to preindustrial levels, which is closely aligned with the observed rise of 1.09 [0.91 to 1.23] °C (Gulev et al., 2021). For the period 1960–1990, the model simulated the northern hemisphere permafrost area at 16.8 [16.7 to 16.9] million km^2, which falls within the reconstructed range of 12.0 to 18.2 million km^2 (Chadburn et al., 2017) and the observation derived extent of 12.21 to 16.98 million km^2 (Zhang et al., 2000). Additionally, the modeled soil carbon stock in the top 3.35 m of permafrost regions for this same period was 1034 [919 to 1151] PgC, with 483 [382 to 587] PgC classified as perennially frozen carbon, accounting for 47% [42% to 51%] of the total permafrost soil carbon stock, in agreement with Hugelius et al. (2014). From 2010 to 2019, the model estimated that anthropogenic carbon emissions were distributed as follows: 5.5 [5.4 to 5.6] PgC yr^{-1} to the atmosphere, 3.0 [2.98 to 3.03] PgC yr^{-1} to the ocean, and 2.5 [2.4 to 2.6] PgC yr^{-1} to terrestrial ecosystems. These estimates are broadly consistent with the global anthropogenic CO_2 budget assessment by the Global Carbon Project (GCP) with figures of 5.1±0.02 PgC yr^{-1} for the atmosphere, 2.5±0.6 PgC yr^{-1} for the ocean, and 3.4±0.9 PgC yr^{-1} for terrestrial ecosystems (Friedlingstein et al., 2020)."

The perturbed parameter approach is described at the end of Section "2.2 Experimental design". We have refined the description to improve coherence. Additionally, we have added a figure to illustrate the probability distribution functions of the four perturbed key permafrost carbon parameters (Figure 2). The revised text and added figure are as follows:

"The Latin hypercube sampling method (McKay et al., 1979) was used to explore the effects of parameter uncertainty on projections of permafrost carbon change. In this study, the probability distribution function of each key permafrost carbon parameter was divided into 25 intervals of equal probability. One value was randomly selected from each interval for a given parameter, and then randomly matched with values of the other three key parameters selected in the same manner to generate parameter sets. This sampling procedure was repeated 10 times, resulting in 250 unique parameter sets (i.e., 250 model variants). For each parameter set, the UVic ESCM v2.10 was first run through a 10,000-year spin-up phase under pre-industrial conditions to achieve a quasi-equilibrium state. For these spin-up runs, the atmospheric CO_2 concentration was fixed at 284.7 ppm and the solar constant was set to 1360.747 W m^{-2}. Following the spin-up, emission-driven transient experiments were conducted under the stabilization, overshoot and

SSP5-8.5 scenarios. The results are presented as the median across all model variants, with uncertainty quantified as the range between the 5th to the 95th percentiles."

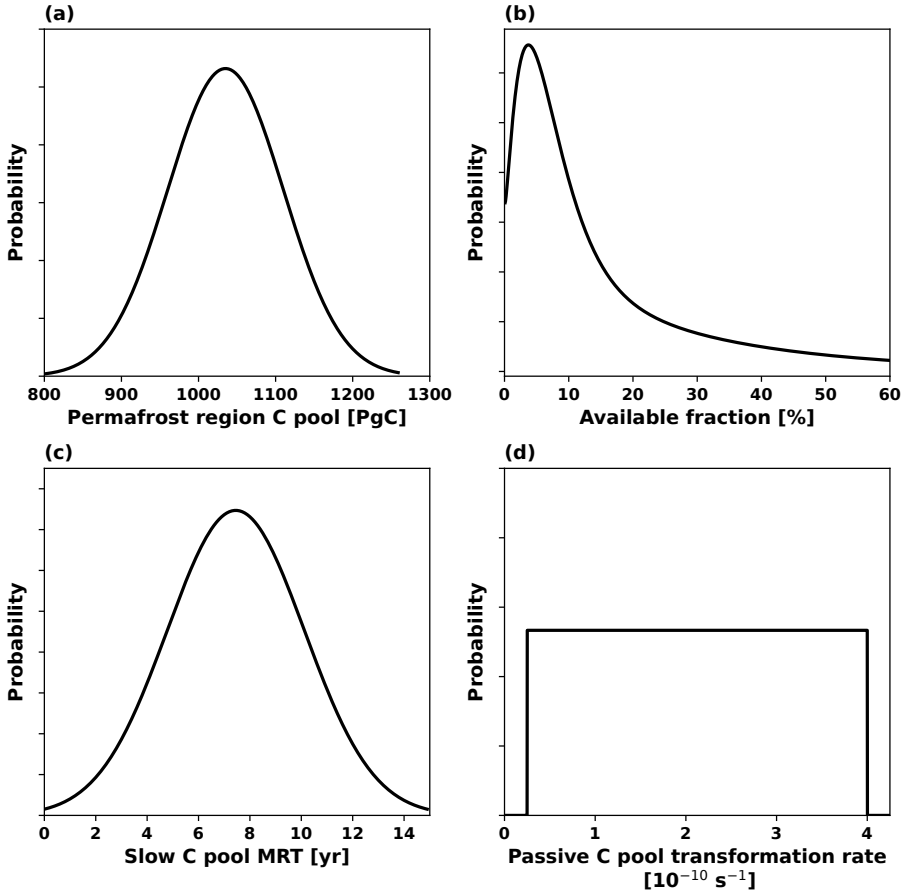

Figure 2. Probability distribution functions of the four key permafrost carbon parameters perturbed in the UVic ESCM v2.10 to represent uncertainty in permafrost carbon response. Panel (d) employs a logarithmic scale on the horizontal axis to better illustrate the distribution of the corresponding parameter. This figure is reproduced from MacDougall (2021).

Line 129 – 136: More clarity is needed about this aspect of the method and the interaction with any permafrost feedback loops. It appears these experiments were done to create drivers for the overshoot scenarios (i.e. the proportional control scheme is not active when the final model runs for analysis are done). It then appears based on this text and the text in section 3.2 that any permafrost carbon fluxes would be tacked onto the emissions and removals needed to accomplish these scenarios. Significant edits are needed here for clarity. The additional warming in Figure 5 also appears well-suited for additional discussion.

Thank you for your detailed comments. Actually, the proportional control scheme was used only in the initial set of simulations, which were conducted to generate CO_2 emission trajectories that follow the intended warming pathways of each scenario (Fig. 1a). These emission trajectories were then used to drive the formal experiments for both stabilization and overshoot scenarios, without any further application of the proportional control scheme during the final model integrations.

To isolate the contribution of permafrost carbon feedback, we conducted two parallel sets of formal experiments for each scenario, both driven by the same CO_2 emission trajectories. The only difference between these sets lies in whether the permafrost carbon module was activated. As you noted, any permafrost carbon fluxes would be tacked onto the emissions and removals needed to accomplish these scenarios. To avoid confusion between scenario names and experiment types, we have introduced distinct suffixes to denote the inclusion or exclusion of permafrost carbon feedback. Specifically, the suffix "-pc" refers to experiments with the permafrost carbon module enabled, while "-npc" refers to those with the module disabled.

To improve clarity, we have revised the relevant section as follows:

"To isolate the contribution of permafrost carbon feedback, two parallel sets of formal experiments were conducted for each scenario, both driven by the same CO_2 emission trajectories. One set included the permafrost carbon module, with experiments designated as SWL-1.5-pc, OS-2-pc, SWL-2-pc, OS-3-pc, SWL-3-pc, OS-4-pc, and SWL-4-pc. The other set disabled the permafrost carbon module and is referred to as SWL-1.5-npc, OS-2-npc, SWL-2-npc, OS-3-npc, SWL-3-npc, OS-4-npc, and SWL-4-npc. Notably, the emission trajectories used in these experiments were derived from initial simulations in which the proportional control scheme was applied to achieve the desired temperature pathways. Once these emission trajectories were established, they were used to drive the formal experiments without further application of the proportional control scheme. Since the emissions trajectories were generated using the UVic ESCM v2.10 without the permafrost carbon module, applying them in simulations with the permafrost module enabled results in any permafrost carbon fluxes being effectively added on top of the pre-derived emissions, thereby causing additional warming. In other words, to achieve the intended climate targets under the same emission pathways, removals equivalent to the permafrost carbon emissions would be required. Therefore, the comparison between these two experiment sets provides a robust framework for quantifying the permafrost carbon feedback under stabilization and overshoot scenarios."

We have also revised the first paragraph of Section 3.2 on radiative impacts of permafrost carbon release to better clarify the expression of additional warming. The revised text is as follows:

"The permafrost carbon release would increase global mean radiative forcing and surface temperature. By comparing two parallel sets of experiments with and without the permafrost carbon module, we were able to quantify the additional radiative forcing and warming caused by permafrost carbon release."

In Section "4 Conclusions and Discussion", we have added a paragraph on the additional warming caused by the permafrost carbon release and its implications on CO_2 emission budgets, as follows:

"Different permafrost carbon release and associated additional warming under overshoot scenarios confirm the path-dependent fate of permafrost region carbon (Kleinen and Brovkin, 2018) and the path-dependent reductions in CO_2 emission budgets (MacDougall et al., 2015; Gasser et al., 2018). As the permafrost carbon was accumulated very slowly during the last millions of years, its release would be tacked onto the anthropogenic CO_2 emissions, and the resulting additional warming

poses a challenge to achieving global climate goals by substantially reducing the remaining carbon budget compatible with the Paris Agreement (MacDougall et al., 2015; Natali et al., 2021). In the overshoot scenarios simulated in this study, permafrost carbon release by 2300 ranges from 60 [35 to 86] PgC to 96 [63 to 135] PgC. The associated additional warming caused by the release ranges from 0.10 [0.06 to 0.15] °C to 0.18 [0.11 to 0.25] °C. This permafrost carbon feedback contributes a substantial addition on top of 1.5 °C warming target under overshoot scenarios, and the magnitude of this additional warming rises with the amplitude of overshoot. To accomplish the 1.5 °C target under the OS-2, OS-3, and OS-4 scenarios, anthropogenic carbon emissions would be reduced by amounts equivalent to the permafrost carbon release. The proportion of carbon removal required to offset permafrost emissions is estimated at 4.9 [2.9 to 7.1] %, 6.5 [4.1 to 9.2] %, and 8.3 [5.4 to 11.5] % by 2300, respectively. Our findings are consistent with previous research utilizing the Monte Carlo ensemble method to evaluate the response of permafrost carbon and its influence on CO_2 emission budgets under overshoot scenarios targeting a 1.5 °C warming limit (Gasser et al., 2018). Specifically, for overshoot amplitudes of 0.5 °C (peak warming of 2 °C) and 1 °C (peak warming of 2.5 °C), the reductions in anthropogenic CO_2 emissions due to permafrost are estimated to be 130 (with a range of 30–300) $PgCO_2$ and 210 (with a range of 50–430) $PgCO_2$, respectively, to meet the long-term 1.5 °C target (Gasser et al., 2018). These results are comparable to our estimates of 60 [35 to 86] PgC under OS-2 and 78 [50 to 111] PgC under OS-3. The differences between the two studies may be partly attributed to differences in the warming trajectories to achieve the same 1.5 °C target. Our study further confirms that if negative CO_2 emissions were to be used to reverse the anthropogenic climate change, the delayed permafrost carbon release would reduce its effectiveness (MacDougall, 2013; Tokarska and Zickfeld, 2015).

Line 159 – 169: I appreciate the perturbed parameter approach that's been taken here. It's presented well as uncertainty bounds in the text but includes some cues about the quantity of runs used and uncertainty bounds in more key figures would highlight it. Moreover, I recommend some discussion of any overlapping trajectories given the range of parameter uncertainty. Otherwise, these aspects of the manuscript may not be as apparent to the reader.

Thank you for your valuable suggestion. We have included the uncertainty bounds in the figures showing changes in GSAT, permafrost area, permafrost carbon loss and permafrost region soil carbon loss (Figure 2 in the original manuscript, Figure 3 in the revised manuscript); changes in permafrost carbon inputs and decomposition, as well as permafrost region soil carbon inputs and decomposition (Figure 4 in the original manuscript, Figure 5 in the revised manuscript); and additional changes in radiative forcing, GSAT warming and permafrost area due to permafrost carbon-climate feedback (Figure 5 in the original manuscript, Figure 7 in the revised manuscript) under overshoot and stabilization scenarios.

To facilitate the discussion of overlapping trajectories of the permafrost carbon, we have expanded the paragraph on the assessment of the relative importance of perturbed model parameters for permafrost region soil carbon release. In addition, we have placed this paragraph in Section "3.1 Permafrost Response" to enhance content coherence. The expanded paragraph reads as follows:

"The uncertainty in permafrost region soil carbon release is nearly the same as that of permafrost carbon release (Fig. 3c, d). For example, the 5th to 95th percentile ranges of permafrost region soil

carbon release under the OS-2 and OS-4 scenarios are 58 PgC and 81 PgC respectively, compared to 52 PgC and 72 PgC for permafrost carbon release. This indicates that the uncertainty in permafrost region soil carbon release is largely driven by the uncertainty in permafrost carbon release. Therefore, we evaluate the relative importance of perturbed permafrost carbon parameters on permafrost region soil carbon release under different temperature pathways through calculating their correlations across all ensemble simulations. In the SSP5-8.5, OS-4, and SWL-4 scenarios, the influence of model parameters on the uncertainty of permafrost carbon losses by 2300 is relatively consistent, with the strongest correlations observed for the permafrost passive carbon pool transformation rate (R=0.81~0.85), followed by the initial quantity of permafrost region soil carbon (R=0.55~0.61). This finding aligns with Ji et al. (2024), which highlights the critical role of these two parameters in the uncertainty of permafrost region soil carbon loss under temperature overshoot and 1.5 °C warming stabilization scenarios."

We have added a discussion of overlapping trajectories in the relevant quantities and explained the overlaps with the aid of the relative importance of perturbed parameters. The added discussion of the overlapping trajectories reads as follows:

"The uncertainty represented by perturbed model parameters for each scenario can be interpreted as model uncertainty. We note that model uncertainty in permafrost carbon release gradually increases with the peak warming level and the duration of overshoot for each scenario (Fig. 3c). However, the uncertainty ranges in permafrost carbon release for overshoot and stabilization scenarios with adjacent warming levels, such as OS-2, SWL-1.5 and SWL-2, substantially overlap. This is especially evident in low-level warming scenarios, where the uncertainty in projected permafrost carbon release is mainly driven by model uncertainty due to parameter perturbations, rather than scenario-related uncertainty. Given the significant roles of the permafrost passive carbon pool transformation rate and the initial quantity of permafrost region soil carbon in determining the uncertainty of permafrost region soil carbon release, it is expected that these two parameters contribute significantly to the overlapping uncertainty ranges of permafrost carbon and permafrost region soil carbon losses across different warming levels. Due to the interaction with soil carbon inputs, the overlapping uncertainty in permafrost region soil carbon release tends to differ from that of permafrost carbon release. For example, the uncertainty ranges in permafrost carbon release under OS-4 and SSP5-8.5 scenarios show considerable overlap (Fig. 3c), but the same does not apply to permafrost region soil carbon release (Fig. 3d), which results from significant differences in soil carbon inputs under distinct CO_2 fertilization backgrounds. The large overlapping uncertainty in projecting permafrost carbon release under low-level warming scenarios, as shown in this study and in previous research (MacDougall, 2015; MacDougall and Knutti, 2016; Gasser et al., 2018), constitutes a significant challenge in accurately estimating the remaining carbon budgets."

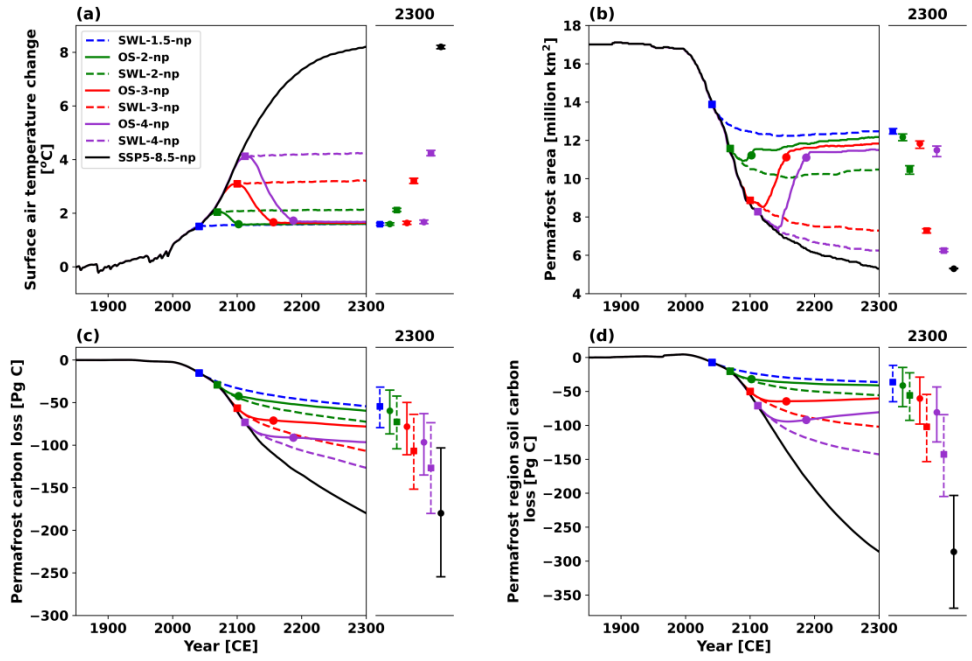

Figure 3. Timeseries of annual mean (a) GSAT changes, (b) permafrost area, (c) permafrost carbon loss and (d) permafrost region soil carbon loss under overshoot (solid lines) and stabilization (dashed lines) scenarios at 1.5 °C (blue), 2.0 °C (green), 3.0 °C (red), and 4 °C (purple) GWLs, as well as the SSP5-8.5 scenario. Square markers indicate the time points when the temperature overshoot reaches its peak or stabilized warming begins, while circle markers indicate when the temperatures return to 1.5 °C in the overshoot scenarios. All changes are relative to the pre-industrial period (1850-1900). Results represent the ensemble median of 250 simulations. Dots on the right panels represent values in the year 2300, with uncertainty ranges estimated as the 5th to 95th percentiles.

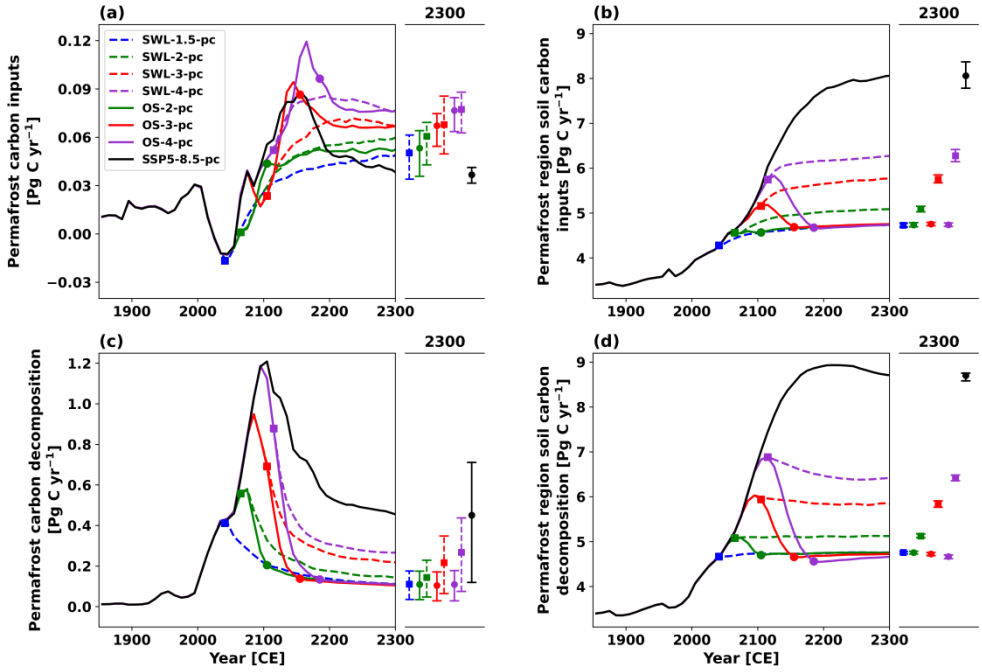

Figure 5. Timeseries of (a) permafrost carbon inputs, (b) permafrost region soil carbon inputs, (c) permafrost carbon decomposition and (d) permafrost region soil carbon decomposition, under the overshoot (solid lines) and stabilization (dashed lines) scenarios at 1.5 °C (blue), 2.0 °C (green), 3.0 °C (red) and 4 °C (purple) GWLs, along with the SSP5-8.5 scenario (black). Square markers indicate the time points when the temperature overshoot reaches its peak or stabilized warming begins, while circle markers indicate when the temperatures return to 1.5 °C in the overshoot scenarios. Results represent the ensemble median of 250 simulations. Dots on the right panels represent values in the year 2300, with uncertainty ranges estimated as the 5th to 95th percentiles.

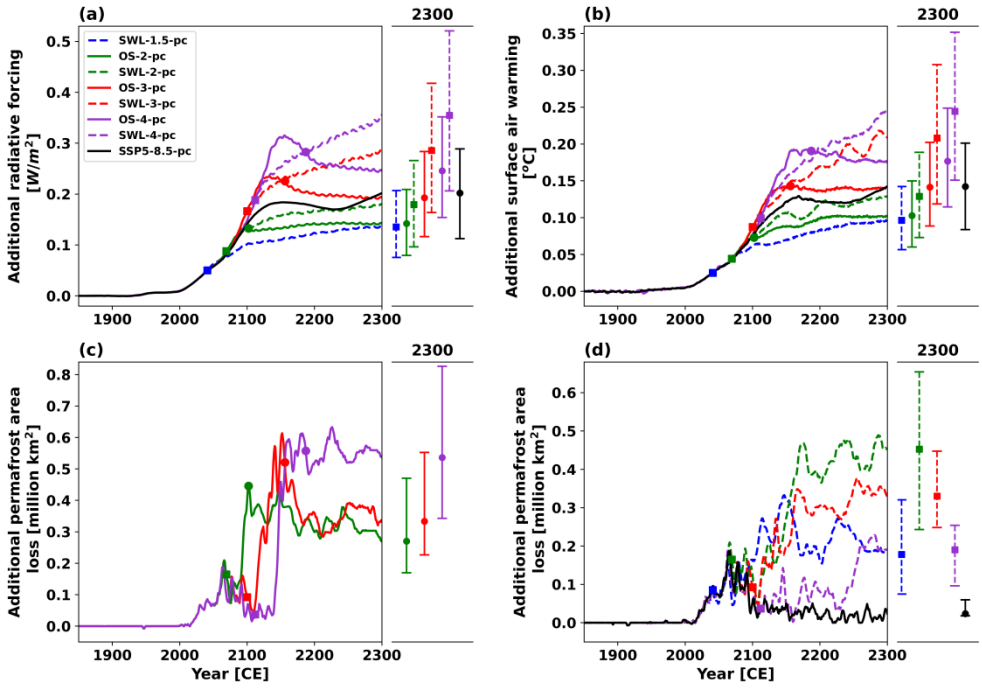

Figure 7. Additional changes in (a) radiative forcing, (b) global mean surface air warming and (c, d) permafrost area due to permafrost carbon-climate feedback in the the overshoot (solid lines) and stabilization (dashed lines) scenarios at 1.5 °C (blue), 2.0 °C (green), 3.0 °C (red) and 4 °C (purple) GWLs, along with the SSP5-8.5 scenario (black). Square markers indicate the time points when the temperature overshoot reaches its peak or stabilized warming begins, while circle markers indicate when the temperatures return to 1.5 °C in the overshoot scenarios. Results represent the ensemble median of 250 simulations. Dots on the right panels represent values in the year 2300, with uncertainty ranges estimated as the 5th to 95th percentiles. In panel (a), the additional radiative forcing is calculated using the simplified expressions (Etminan et al., 2016) based on simulated CO_2 concentrations. In panels (c) and (d), the additional permafrost area loss is smoothed using a 5-year rolling average to eliminate shorter interannual variability.

Line 200: Greater elaboration on this result could be valuable. Assessing this impact at the year 2300 seems reasonable, however, given enough time will all the overshoot scenarios eventually converge with SWL-1.5?

We sincerely appreciate your valuable suggestion. To further investigate whether all overshoot scenarios eventually converge with SWL-1.5, we have extended the SWL-1.5 and overshoot

simulations to the year 2400 and compared the permafrost carbon inputs, decomposition and surface climate between them post-overshoot (Figure R2). A new paragraph has been added to Section "4 Conclusions and Discussion" to elaborate on this point and help readers better understand the model's long-term behavior. The added discussion reads as follows:

"The permafrost carbon under overshoot scenarios shows a certain degree of recovery relative to the stabilization scenario of SWL-1.5 (Fig. 4b). It is therefore of interest to assess whether the permafrost carbon under overshoot scenarios will eventually converge with that under SWL-1.5. To better explore this question, we extended the SWL-1.5 and overshoot simulations to year 2400 (data not shown). The permafrost carbon inputs are larger under overshoot scenarios than SWL-1.5, while the permafrost carbon decomposition shows much smaller differences between the two. This tends to indicate that the smaller permafrost carbon stocks under overshoot scenarios in 2300 would eventually catch up to the levels under SWL-1.5. To test this hypothesis, we estimate the time required to reach convergence by the ratio between the difference in permafrost carbon stocks and the difference in net permafrost carbon inputs (i.e., annual permafrost carbon inputs minus decomposition) for the overshoot scenarios relative to the SWL-1.5 scenario. Based on simulation outputs for the year 2300, the estimated median times for OS-2, OS-3 and OS-4 to catch up permafrost carbon with SWL-1.5 are 1076, 1008 and 1433 years, respectively. When based on outputs from the year 2400, the corresponding estimates increase to 1377, 1199 and 1568 years. This means that convergence would take even longer if estimated from later simulation years, mainly due to gradually weakened permafrost carbon inputs. The relatively larger permafrost carbon inputs under overshoot scenarios result not only from warmer climates during the stabilization period, but also from increased litterfall during the overshoot phase. This extra litterfall gradually moves through the active layer and is transported to the permafrost zone. Over time, however, the effect of this extra litterfall gradually diminishes, leading to a reduction in permafrost carbon inputs. Consequently, it may take extremely long timescales for the overshoot scenarios to fully converge with SWL-1.5 in terms of permafrost carbon stocks. In addition, the additional permafrost carbon release during the temperature overshoot period leads to greater additional warming under overshoot scenarios than the SWL-1.5 scenario, and this enhanced warming persists until the year 2400 without significant decline. Greater soil carbon loss under overshoot conditions also substantially alters the hydrological and thermal properties of soil, affecting the processes that govern carbon cycling. These persistent changes in surface climate and soil properties might stabilize the carbon, water, and energy cycles at alternative equilibria after overshoot through the interactions between physical and biophysical processes (de Vrese and Brovkin, 2021). Therefore, the overshoot scenarios might ultimately fail to converge to SWL-1.5 scenario in terms of permafrost carbon stocks."

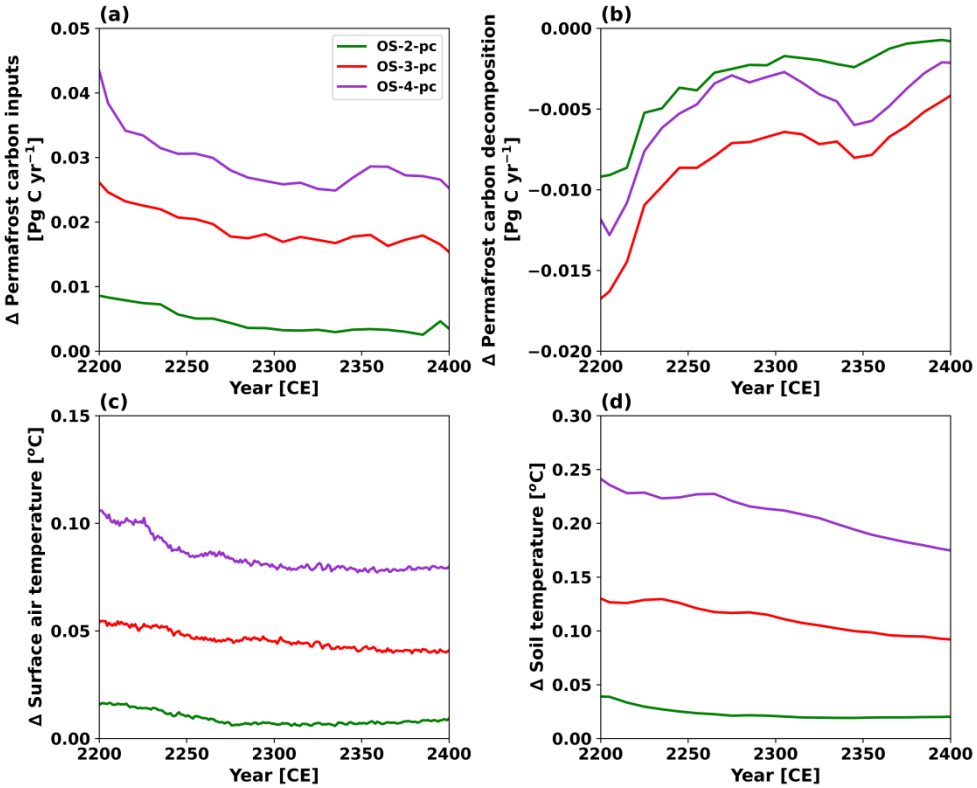

Figure R2. Timeseries of changes in (a) permafrost carbon inputs, (b) permafrost carbon decomposition, (c) GSAT and (d) soil temperature in permafrost regions under overshoot scenarios (OS-2-pc, OS-3-pc, OS-4-pc) from the year 2200 to 2400. All variables are shown as anomalies relative to the SWL-1.5 scenario. Panel (d) shows the regional average of soil temperature in permafrost regions, averaged over the top 3.35 m of soil.

Line 220 and throughout: There is a substantial body of literature related to the response of arctic vegetation to climate change and the processes represented therein. Providing the reader with additional information on the vegetation model within UVICC ESM, the processes represented, limitations therein, including some information about the response of vegetation productivity and framing these results in that context would enhance their presentation. Additional background on the permafrost model would add additional clarity as to why permafrost carbon inputs do not appear to follow the same trajectory as soil carbon.

Thank you for your suggestion. We have expanded the background information on the vegetation model within UVic ESCM as follows:

"The terrestrial component uses the Top-down Representation of Interactive Foliage and Flora Including Dynamics (TRIFFID) vegetation model to describe the states of five plant functional types (PFT): broadleaf tree, needleleaf tree, C3 grass, C4 grass, and shrub (Cox, 2001; Meissner et al., 2003). A coupled photosynthesis-stomatal conductance model is used to calculate carbon uptake via photosynthesis, which is subsequently allocated to vegetation growth and respiration. The resulting net carbon fluxes drive changes in vegetation characteristics, including areal coverage, leaf area index, and canopy height for each PFT. The UVic ESCM v2.10 utilized in this

study does not account for nutrient limitations in the terrestrial carbon cycle, leading to an overestimation of global gross primary productivity and an enhanced capacity of land to take up atmospheric carbon (De Sisto et al., 2023). However, the model reasonably represents the dominant PFTs of C3 grass, shrub and needleleaf tree at northern high latitudes, although it underestimates vegetation carbon density over this area (Mengis et al., 2020)."

We have also added the response of vegetation productivity in Section "3 Results" to better understanding permafrost region soil carbon inputs as following:

"The permafrost region soil carbon inputs generally track the trajectory of litter flux across the same area, with an approximate delay of 10-20 years (now shown). To attribute the contribution of permafrost region soil carbon inputs, we examined how dominant vegetation types (needleleaf tree, C3 grass and shrub) over the permafrost region adapt to temperature and atmospheric CO_2 concentrations in both overshoot and stabilization scenarios (Figure 6). Needleleaf trees expand slowly and continuously in the permafrost region in both overshoot and stabilization scenarios, while the areal coverage of shrubs closely follows the trajectory of GSAT. The combined areal coverage of trees and shrubs is projected to cover about 62% upon 1.5 °C warming relative to pre-industrial levels around 2040s, slightly higher than the 24-52% range projected for 2050 using a statistical approach that links climate conditions to vegetation types under two distinct emission trajectories (Pearson et al., 2013). During the warming and cooling phases of overshoot scenarios, the expansion and reduction of shrubs correspond with the degradation and expansion of C3 grasses, respectively. Among the three dominant PFTs, only shrubs show a nearly reversible response in areal coverage, net primary productivity (NPP) and vegetation carbon with respect to GSAT under overshoot scenarios. In contrast, the continuous reduction of C3 grasses and the expansion of needleleaf trees suggest a degree of irreversibility in the structure and vegetation carbon density of northern high latitude terrestrial ecosystems under overshoot scenarios. This contrasts with a previous study that employed prescribed vegetation distributions, which reported only minor differences in vegetation carbon after the overshoots compared to the reference simulation with no overshoot (Schwinger et al., 2022). In our study, the shifts in vegetation composition and changes in living biomass, especially those associated with woody vegetation, are key drivers of permafrost region soil carbon inputs."

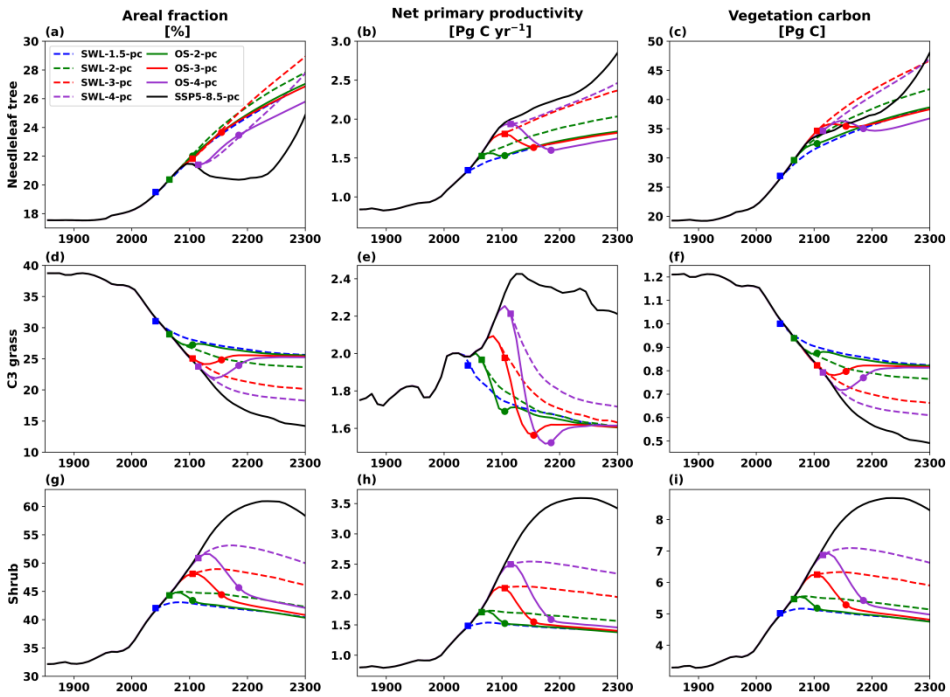

Figure 6. Timeseries of annual mean areal fraction (left column), net primary productivity (middle column) and vegetation carbon (right column) under overshoot (solid lines) and stabilization (dashed lines) scenarios at 1.5 °C (blue), 2.0 °C (green), 3.0 °C (red), and 4 °C (purple) GWLs, as well as the SSP5-8.5 scenario (black). Each row represents one of the three dominant plant functional type (PFT): (a-c) needleleaf tree, (d-f) C3 grass and (g-i) shrub. Square markers indicate the time points when the temperature overshoot reaches its peak or stabilized warming begins, while circle markers indicate when the temperatures return to 1.5 °C in the overshoot scenarios. Results represent the ensemble median of 250 simulations, and the uncertainty is not displayed due to the small range.

To explain why permafrost carbon inputs do not follow the same trajectory as soil carbon, especially under overshoot scenarios, we emphasized that in the model, litterfall is allocated to soil layers with temperatures above 1 °C according to an exponentially decreasing function of depth. When all soil layers are below 1 °C, organic carbon from the litterfall is added to the top soil layer. Meanwhile, permafrost carbon and non-permafrost soil carbon are both represented as depth-resolved carbon pools within the top six soil layers. The movement of permafrost carbon due to cryoturbation mixing is parameterized as being proportional to the gradient of total soil carbon with depth. Soil carbon that diffuses downward through the permafrost table is converted to permafrost carbon. During the cooling phase of overshoot scenarios, increased litterfall and a rising permafrost table lead to elevated carbon concentrations in surface soil layers, resulting in a surge in permafrost carbon inputs. Conversely, under the SSP5-8.5 scenario, permafrost carbon inputs only show a minor peak. This is due to the continuous reduction in permafrost area and the deepening of the permafrost table, both of which reduce carbon concentrations in the upper soil layers and weaken vertical diffusion, despite the increasing litter flux under a strong CO_2 fertilization background. We note that the approach adopted in the model may not accurately reflect natural processes of vertical carbon movement, which are influenced by soil porosity heterogeneity, freeze-thaw cycles, and ice expansion upon freezing.

Minor comments:

Abstract: for clarity suggest reducing the use of acronyms in the abstract and possibly parts of the text.

Thank you for your suggestion. In response to your suggestion, we have reduced the use of acronyms in the abstract and replaced "SWL" and "OS" with their full terms, "stabilization" and "overshoot." We will continue to review acronym usage throughout the manuscript to ensure clarity and accessibility.

Line 25: gradual and abrupt seem to refer to the rate of carbon loss suggest revision to distinguish this from the processes of gradual and abrupt thaw.

Thank you for your suggestion. We have revised the wording to ensure that gradual and abrupt explicitly refer to the thawing processes. Line 25 has been changed to “gradual or abrupt permafrost thaw, along with subsequent microbial decomposition, would release carbon dioxide (CO_2) and methane (CH_4) into the atmosphere...”.

Line 50: suggest adding further discission of the mechanism behind the presence or absence of hysteresis behavior in different processes as this is useful background.

Thank you for this insightful suggestion. We agree that a more detailed discussion of the mechanism behind the presence or absence of hysteresis behavior in different processes would strengthen the background of our study. To address this, we have expanded the discussion in this section by highlighting key factors influencing hysteresis in permafrost carbon dynamics, including thermophysical inertia, microbial decomposition lag, and hydrological feedbacks.

The revised text now reads: “Additionally, a temporary warming of the permafrost regions entails important legacy effects and lasting impacts on their physical state and carbon cycle under various overshoot levels. The presence or absence of hysteresis effect in these processes is influenced by multiple factors, including the thermal inertia of permafrost soils, potential shifts in vegetation composition, and varying levels of compensation between irreversible permafrost carbon losses and gains in vegetation and non-permafrost soil carbon reservoirs (MacDougall, 2013; Schwinger et al., 2022). Furthermore, the soil carbon loss under overshoot scenarios significantly affects the hydrological and thermal properties of soils, which in turn modulate the processes involved. The interactions between physical and biophysical processes can potentially stabilize the carbon, water, and energy cycles at distinct post-overshoot equilibria (de Vrese and Brovkin, 2021).”

Line 229: Suggest clarifying the timescale being discussed in this summary information. It reads very similarly to the sentence immediately prior.

Thank you for the suggestion. We have revised this section to improve clarity and to specify the timescale. The revised manuscript is as follows:

“In all overshoot and stabilization scenarios simulated in this study, the permafrost region soil serves as a net carbon source for atmospheric CO_2 by 2300. However, during the stabilization phase of OS-3 and OS-4 (Fig. 2d), the permafrost region soil turns into a carbon sink, as soil carbon inputs surpass the reduced decomposition activity due to the depletion of soil carbon stocks and reduced warming levels.”

References

Avis, C. A., Weaver, A. J., and Meissner, K. J.: Reduction in areal extent of high-latitude wetlands in response to permafrost thaw, Nature Geoscience, 4, 444–448, https://doi.org/10.1038/ngeo1160, 2011.

Chadburn, S. E., Burke, E. J., Cox, P. M., Friedlingstein, P., Hugelius, G., and Westermann, S.: An observation-based constraint on permafrost loss as a function of global warming, Nature Climate Change, 7, 340 – 344, https://doi.org/10.1038/nclimate3262, 2017.

Cox, P.: Description of the TRIFFID dynamic global vegetation model. Hadley Centre Technical., 24, 1 – 16, 2001.

De Sisto, M. L., MacDougall, A. H., Mengis, N., and Antoniello, S.: Modelling the terrestrial nitrogen and phosphorus cycle in the UVic ESCM, Geoscientific Model Development, 16, 4113 – 4136, https://doi.org/10.5194/gmd-16-4113-2023, 2023.

De Vrese, P. and Brovkin, V.: Timescales of the permafrost carbon cycle and legacy effects of temperature overshoot scenarios, Nature Communications, 12, 2688, https://doi.org/10.1038/s41467-021-23010-5, 2021.

Etminan, M., Myhre, G., Highwood, E. J., and Shine, K. P.: Radiative forcing of carbon dioxide, methane, and nitrous oxide: A significant revision of the methane radiative forcing, Geophysical Research Letters, 43, https://doi.org/10.1002/2016GL071930, 2016.

Friedlingstein, P., O’Sullivan, M., Jones, M. W., Andrew, R. M., Hauck, J., Olsen, A., Peters, G. P., Peters, W., Pongratz, J., Sitch, S., Le Quéré, C., Canadell, J. G., Ciais, P., Jackson, R. B., Alin, S., Aragão, L. E. O. C., Arneth, A., Arora, V., Bates, N. R., Becker, M., Benoit-Cattin, A., Bittig, H. C., Bopp, L., Bultan, S., Chandra, N., Chevallier, F., Chini, L. P., Evans, W., Florentie, L., Forster, P. M., Gasser, T., Gehlen, M., Gilfillan, D., Gkritzalis, T., Gregor, L., Gruber, N., Harris, I., Hartung, K., Haverd, V., Houghton, R. A., Ilyina, T., Jain, A. K., Joetzjer, E., Kadono, K., Kato, E., Kitidis, V., Korsbakken, J. I., Landschützer, P., Lefèvre, N., Lenton, A., Lienert, S., Liu, Z., Lombardozzi, D., Marland, G., Metzl, N., Munro, D. R., Nabel, J. E. M. S., Nakaoka, S.-I., Niwa, Y., O’Brien, K., Ono, T., Palmer, P. I., Pierrot, D., Poulter, B., Resplandy, L., Robertson, E., Rödenbeck, C., Schwinger, J., Séférian, R., Skjelvan, I., Smith, A. J. P., Sutton, A. J., Tanhua, T., Tans, P. P., Tian, H., Tilbrook, B., van der Werf, G., Vuichard, N., Walker, A. P., Wanninkhof, R., Watson, A. J., Willis, D., Wiltshire, A. J., Yuan, W., Yue, X., and Zaehle, S.: Global Carbon Budget 2020, Earth System Science Data, 12, 3269 – 3340, https://doi.org/10.5194/essd-12-3269-2020, 2020.

Gasser, T., Kechiar, M., Ciais, P., Burke, E. J., Kleinen, T., Zhu, D., Huang, Y., Ekici, A., and Obersteiner, M.: Path-dependent reductions in CO2 emission budgets caused by permafrost carbon release, Nature Geoscience, 11, 830 – 835, https://doi.org/10.1038/s41561-018-0227-0, 2018.

Gulev, S. K., Thorne, P. W., Ahn, J., Dentener, F. J., Domingues, C. M., Gerland, S., Gong, D., Kaufman, D. S., Nnamchi, H. C., Quaas, J., Rivera, J. A., Sathyendranath, S., Smith, S. L., Trewin, B., von Schuckmann, K., Vose, R. S., Allan, R., Collins, B., Turner, A., and Hawkins, E.: Changing state of the climate system, edited by: Masson-Delmotte, V., Zhai, P., Pirani, A., Connors, S. L., Péan, C., Berger, S., Caud, N., Chen, Y., Goldfarb, L., Gomis, M. I., Huang, M., Leitzell, K., Lonnoy, E., Matthews, J. B. R., Maycock, T. K., Waterfield, T., Yelekçi, O., Yu, R., and Zhou, B., Cambridge University Press, Cambridge, UK, 287 – 422, 2021.

Hugelius, G., Strauss, J., Zubrzycki, S., Harden, J. W., Schuur, E. a. G., Ping, C.-L., Schirrmeister, L., Grosse, G., Michaelson, G. J., Koven, C. D., O'Donnell, J. A., Elberling, B., Mishra, U., Camill, P., Yu, Z., Palmtag, J., and Kuhry, P.: Estimated stocks of circumpolar permafrost carbon with quantified uncertainty ranges and identified data gaps, Biogeosciences, 11, 6573–6593, https://doi.org/10.5194/bg-11-6573-2014, 2014.

Kleinen, T. and Brovkin, V.: Pathway-dependent fate of permafrost region carbon, Environmental Research Letters, 13, 094001, https://doi.org/10.1088/1748-9326/aad824, 2018.

Koven, C., Friedlingstein, P., Ciais, P., Khvorostyanov, D., Krinner, G., and Tarnocai, C.: On the formation of high-latitude soil carbon stocks: Effects of cryoturbation and insulation by organic matter in a land surface model, Geophysical Research Letters, 36, https://doi.org/10.1029/2009GL040150, 2009.

MacDougall, A. H.: Reversing climate warming by artificial atmospheric carbon-dioxide removal: Can a Holocene-like climate be restored? Geophysical Research Letters, 40, 5480 – 5485, https://doi.org/10.1002/2013GL057467, 2013.

MacDougall, A. H., Zickfeld, K., Knutti, R., and Matthews, H. D.: Sensitivity of carbon budgets to permafrost carbon feedbacks and non-CO2 forcings, Environmental Research Letters, 10, 125003, https://doi.org/10.1088/1748-9326/10/12/125003, 2015.

MacDougall, A. H. and Knutti, R.: Projecting the release of carbon from permafrost soils using a perturbed parameter ensemble modelling approach, Biogeosciences, 13, 2123–2136, https://doi.org/10.5194/bg-13-2123-2016, 2016.

MacDougall, A. H.: Estimated effect of the permafrost carbon feedback on the zero emissions commitment to climate change, Biogeosciences, 18, 4937–4952, https://doi.org/10.5194/bg-18-4937-2021, 2021.

McKay, M. D., Beckman, R. J., and Conover, W. J.: A Comparison of Three Methods for Selecting Values of Input Variables in the Analysis of Output from a Computer Code, Technometrics, 21, 239 – 245, https://doi.org/10.2307/1268522, 1979.

Meissner, K. J., Weaver, A. J., Matthews, H. D., and Cox, P. M.: The role of land surface dynamics in glacial inception: a study with the UVic Earth System Model, Climate Dynamics, 21, 515–537, https://doi.org/10.1007/s00382-003-0352-2, 2003.

Mengis, N., Keller, D. P., MacDougall, A. H., Eby, M., Wright, N., Meissner, K. J., Oschlies, A., Schmittner, A., MacIsaac, A. J., Matthews, H. D., and Zickfeld, K.: Evaluation of the University of Victoria Earth System Climate Model version 2.10 (UVic ESCM 2.10), Geoscientific Model Development, 13, 4183–4204, https://doi.org/10.5194/gmd-13-4183-2020, 2020.

Natali, S. M., Holdren, J. P., Rogers, B. M., Treharne, R., Duffy, P. B., Pomerance, R., and MacDonald, E.: Permafrost carbon feedbacks threaten global climate goals, Proceedings of the National Academy of Sciences, 118, e2100163118, https://doi.org/10.1073/pnas.2100163118, 2021.

Pearson, R. G., Phillips, S. J., Loranty, M. M., Beck, P. S. A., Damoulas, T., Knight, S. J., and Goetz, S. J.: Shifts in Arctic vegetation and associated feedbacks under climate change, Nature Climate Change, 3, 673 – 677, https://doi.org/10.1038/nclimate1858, 2013.

Schuur, E. a. G., McGuire, A. D., Schädel, C., Grosse, G., Harden, J. W., Hayes, D. J., Hugelius, G., Koven, C. D., Kuhry, P., Lawrence, D. M., Natali, S. M., Olefeldt, D., Romanovsky, V. E., Schaefer, K., Turetsky, M. R., Treat, C. C., and Vonk, J. E.: Climate change and the permafrost carbon feedback, Nature, 520, 171 – 179, https://doi.org/10.1038/nature14338, 2015.

Schwinger, J., Asaadi, A., Steinert, N. J., and Lee, H.: Emit now, mitigate later? Earth system reversibility under overshoots of different magnitudes and durations, Earth System Dynamics, 13, 1641 – 1665, https://doi.org/10.5194/esd-13-1641-2022, 2022.

Strauss, J., Schirrmeister, L., Grosse, G., Fortier, D., Hugelius, G., Knoblauch, C., Romanovsky, V., Schädel, C., Schneider von Deimling, T., Schuur, E. A. G., Shmelev, D., Ulrich, M., and Veremeeva, A.: Deep Yedoma permafrost: A synthesis of depositional characteristics and carbon vulnerability, Earth-Science Reviews, 172, 75 – 86, https://doi.org/10.1016/j.earscirev.2017.07.007, 2017.

Strauss, J., Laboor, S., Schirrmeister, L., Fedorov, A. N., Fortier, D., Froese, D., Fuchs, M., Günther, F., Grigoriev, M., Harden, J., Hugelius, G., Jongejans, L. L., Kanevskiy, M., Kholodov, A., Kunitsky, V., Kraev, G., Lozhkin, A., Rivkina, E., Shur, Y., Siegert, C., Spektor, V., Streletskaya, I., Ulrich, M., Vartanyan, S., Veremeeva, A., Anthony, K. W., Wetterich, S., Zimov, N., and Grosse, G.: Circum-Arctic Map of the Yedoma Permafrost Domain, Frontiers in Earth Science, 9, 758360, https://doi.org/10.3389/feart.2021.758360, 2021.

Strauss, J., Laboor, S., Schirrmeister, L., Fedorov, A. N., Fortier, D., Froese, D. G., Fuchs, M., Günther, F., Grigoriev, M. N., Harden, J. W., Hugelius, G., Jongejans, L. L., Kanevskiy, M. Z., Kholodov, A. L., Kunitsky, V., Kraev, G., Lozhkin, A. V., Rivkina, E., Shur, Y., Siegert, C., Spektor, V., Streletskaya, I., Ulrich, M., Vartanyan, S. L., Veremeeva, A., Walter Anthony, K. M., Wetterich,

S., Zimov, N. S., and Grosse, G.: Database of Ice-Rich Yedoma Permafrost Version 2 (IRYP v2), PANGAEA, https://doi.org/10.1594/PANGAEA.940078, 2022.

Tokarska, K. B. and Zickfeld, K.: The effectiveness of net negative carbon dioxide emissions in reversing anthropogenic climate change, Environmental Research Letters, 10, 094013, https://doi.org/10.1088/1748-9326/10/9/094013, 2015.

Zhang, T., Heginbottom ,J. A., Barry ,R. G., and Brown, J.: Further statistics on the distribution of permafrost and ground ice in the Northern Hemisphere 1, Polar Geography, 24, 126 – 131, https://doi.org/10.1080/10889370009377692, 2000.

Zimov, S. A., Schuur, E. A. G., and Chapin, F. S.: Permafrost and the Global Carbon Budget, Science, 312, 1612 – 1613, https://doi.org/10.1126/science.1128908, 2006.